DOA Estimation for Non-Circular Signal with Nested Array

Jing Zhao, Sheng Liu*, Sihuan Que, Qikui Zou, and Mengmei Ou

Abstract—A direction-of-arrival (DOA) estimation algorithm for non-circular signals with nested array is proposed. A closed formula is given to construct a partitioned fourth-order-cumulant (FOC) matrix by using the FOCs of received data. Then, an improved multiple signal classification (MUSIC) algorithm for non-circular signals (NC-MUSIC) based on FOC is introduced. The proposed algorithm shows higher estimation accuracy and angular resolution than some traditional NC-MUSIC algorithms, especially in the low SNR case. Some simulation experiments are proposed to prove the validity of the proposed algorithm.

1. INTRODUCTION

DOA estimation is one of the main research topics of array signal processing. It is widely applied in many relevant fields, such as radar, wireless communication, and sonar [1–3]. Noncircular signals (e.g., binary phase shift keying (BPSK) and amplitude modulated (AM) signals) are often employed in digital communications due to the improved performance brought by noncircular properties. In [4], a multiple signal classification (MUSIC) algorithm was presented for noncircular signals (called NC-MUSIC). Subsequently, a rooting MUSIC algorithm for noncircular signals (called Root-NC-MUSIC) was proposed in [5]. In [6], an improved NC-MUSIC algorithm aiming the coexistence of both circular and noncircular sources was addressed. However, the performance of this algorithm deteriorates due to the appearance of false peaks. In [7], the authors analyzed the cause for the appearance of false peaks in the method [6] and proposed an improved scheme. In [8], the traditional unitary estimation of signal parameters via rotational invariance technique (UESPRIT) [9] was applied in DOA estimation of noncircular signals (called NC-UESPRIT). In order to reduce the computational burden caused by eigenvalue decomposition (EVD), a propagator algorithm (PM) for noncircular signals (called NC-PM) [10] and rooting propagator algorithm (called Root-NC-PM) [11] were proposed in succession. In [12], a simultaneous singular value decomposition algorithm based on an L-shaped array was proposed for 2D DOA estimation of noncircular signals. Using the FOCs of received data to construct a FOC matrix instead of the covariance matrix formed by the second-order statistics (SOS) is an effective way to extend the array aperture. Many DOA estimation methods based on FOC [13–15] were proposed by scholars. In [15], the authors utilized the FOCs of received data to construct a high-order FOC matrix, and an NC-MUSIC algorithm based on FOC was presented.

However, all these methods mentioned above are designed for uniform linear arrays (ULAs). Compared with a uniform array, a sparse array has many obvious advantages for DOA estimation, such as enhancing spatial resolution and improving estimation accuracy. However, these advantages come out only when the array is designed rationally. There are many effective design methods of sparse arrays, such as minimum redundancy array [16], coprime array [17, 18], and nested array [19–21].

In this paper, an improved nested array [20] is employed to estimate the DOA of noncircular signals. FOCs of received data are used to construct a high-order FOC matrix, and a closed formula

for constructing the FOC matrix is given. Then, an NC-MUSIC algorithm based FOC is derived. Due to further expansion of the aperture, the proposed algorithm has better effect than some classical algorithms in accuracy and angular resolution.

Notation: The operational symbols $[\bullet]^*$, $[\bullet]^T$, $[\bullet]^H$, and $\otimes$ stand for conjugate, transpose, conjugate transpose, and Kronecker product, respectively. $[\mathbf{c}]_{i:j}$ denotes a vector consisting of the ith to the jth elements of vector $\mathbf{c}$.

2. SIGNAL MODEL

The nested array [20] consists of two sub-arrays shown as Fig. 1, where the last sensor of the first subarray is the first sensor of the second subarray. Hence the number of sensors of this array is $N + M - 1$. The sensors of the first array are arranged on the x-axis with coordinates $0, d, \cdots, (N-1)d$, and the sensors of the second array are arranged on the x-axis with coordinates $(N-1)d, 2Nd, \cdots, (MN + M - N - 3)d, (MN + M - 3)d$. Assume that $d = \lambda/2$, where λ is the wavelength of incident signal.
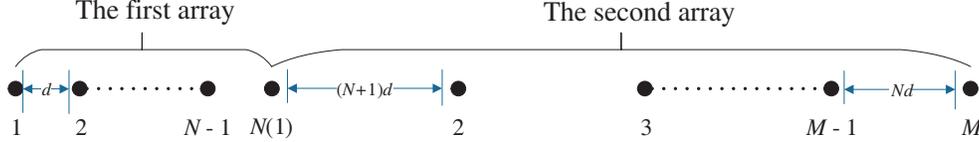
Figure 1. The structure of nested array.

Suppose that K far-field, narrowband, incoherent and non-circular signals $s_1(t), \cdots, s_K(t)$ come from the directions $\theta_1, \theta_2, \cdots, \theta_K$. Denote $\boldsymbol{\theta} = [\theta_1, \theta_2, \cdots, \theta_K]$ and $\Delta = 2\pi d/\lambda$, and the received vectors of two arrays are given by

$$\begin{cases} \mathbf{x}(t) = \mathbf{A}(\boldsymbol{\theta})\mathbf{s}(t) + \mathbf{n}_1(t) \\ \mathbf{y}(t) = \mathbf{B}(\boldsymbol{\theta})\mathbf{s}(t) + \mathbf{n}_2(t) \end{cases} \tag{1}$$

where $\mathbf{x}(t) = [x_1(t), \cdots, x_{N-1}(t), x_N(t)]^T \in C^{N\times1}$, $\mathbf{y}(t) = [y_1(t), \cdots, y_{M-1}(t), y_M(t)]^T \in C^{M\times1}$, $\mathbf{s}(t) = [s_1(t), \cdots, s_K(t)]^T \in C^{K\times1}$ is the non-Gaussian non-circular signal vector; $\mathbf{n}_1(t) = [n_{12}(t), \cdots, n_{2M}(t)]^T \in C^{M\times1}$ and $\mathbf{n}_2(t) = [n_{21}(t), \cdots, n_{2M}(t)]^T \in C^{M\times1}$ are the complex Gaussian noise vectors received by two sub arrays; $\mathbf{A}(\boldsymbol{\theta}) = [\mathbf{a}(\theta_1), \cdots, \mathbf{a}(\theta_K)] \in C^{N\times K}$ with $\mathbf{a}(\theta_k) = [1, \exp(-i\Delta\sin(\theta_k)), \cdots, \exp(-i\Delta(N-1)\sin(\theta_k))]^T$ and $\mathbf{B}(\boldsymbol{\theta}) = [\mathbf{b}(\theta_1), \cdots, \mathbf{b}(\theta_K)] \in C^{M\times K}$ with $\mathbf{b}(\theta_k) = [\exp(-i\Delta(N-1)\sin(\theta_k)), \exp(-i\Delta 2N\sin(\theta_k)), \cdots, \exp(-i\Delta(MN+M-3)\sin(\theta_k))]^T$ are the manifold matrices.

Assume that all the incident signals have the non-circular property. Thus, we can get the conjugate expression of received vectors as [10–12]

$$\begin{cases} \mathbf{x}^*(t) = \mathbf{A}^*(\boldsymbol{\theta})\Phi^*\mathbf{s}(t) + \mathbf{n}_1^*(t) \\ \mathbf{y}^*(t) = \mathbf{B}^*(\boldsymbol{\theta})\Phi^*\mathbf{s}(t) + \mathbf{n}_2^*(t) \end{cases} \tag{2}$$

where $\boldsymbol{\Phi} = \mathrm{diag}\{e^{-j\phi_1}, e^{-j\phi_2}, \cdots, e^{-j\phi_K}\}$, and ϕ_k, $k = 1, 2, \cdots, K$, is the arbitrary phase shift of the kth signal.

Remark: In this paper, we assume that the sensors are isotropic, and ignore the influence of mutual coupling between two sensors. Because the improved nested array [20] has higher degrees of freedom than the other sparse arrays [17, 19] and a more regular array structure than minimum redundancy array [16], we use this array geometry to estimate the DOA of non-circular signals.

3. ALGORITHM DESCRIPTION

3.1. Construction of FOC Matrix

In this subsection, we use the FOCs of received data to construct a FOC matrix which has equivalent function as the covariance matrix. Using the position sum between two sensors, we can get

$N + MN + 2M - 4$ virtual sensors with nonnegative position. Meanwhile, using the position difference between two sensors, we can get $MN + M - 2$ virtual sensors with nonnegative position. In order to cut down the repeated data in FOC matrix and reduce the complexity for dealing with the FOC matrix, we only use the FOCs of received data from some specific sensors.

Firstly, according to the non-circular property of non-circular signals, we denote four FOCs as

$$\begin{cases} cum\{s_k, s_k^*, s_k^*, s_k\} = s_{0k} \\ cum\{s_k^*, s_k^*, s_k^*, s_k\} = e^{j\phi_k} s_{0k} \\ cum\{s_k, s_k^*, s_k, s_k\} = e^{-j\phi_k} s_{0k} \\ cum\{s_k^*, s_k^*, s_k, s_k\} = s_{0k} \end{cases} \quad (3)$$

Then, we construct four FOC matrices $\mathbf{C}_1 \in C^{(MN+M-2)\times(MN+M-2)}$, $\mathbf{C}_2 \in C^{(MN+M-2)\times(MN+2M+N-3)}$, $\mathbf{C}_3 \in C^{(MN+2M+N-3)\times(MN+M-2)}$ and $\mathbf{C}_4 \in C^{(MN+2M+N-3)\times(MN+2M+N-3)}$. Let $C_i(u,v)$ be the element on the uth row and the vth column of $\mathbf{C}_i$.

Denote the unique decomposition of u and v as

$$\begin{cases} u = u_1 + u_2(N+1) \\ v = v_1 + v_2(N+1) \end{cases} \quad (4)$$

where $0 \le u_1, v_1 \le N$. Then, we can construct $\mathbf{C}_1$ by

$$\mathbf{C}_1(u,v) = \begin{cases} cum\{y_M(t), y_{M-u_2}^*(t), y_M^*(t), y_{M-v_2}(t)\}, & \text{when } u_1 = 0, v_1 = 0 \\ cum\{y_{u_2+1}(t), x_{N-u_1+1}^*(t), y_M^*(t), y_{M-v_2}(t)\}, & \text{when } u_1 \ne 0, v_1 = 0 \\ cum\{y_M(t), y_{M-u_2}^*(t), y_{v_2+1}^*(t), x_{N-v_1+1}(t)\}, & \text{when } u_1 = 0, v_1 \ne 0 \\ cum\{y_{u_2+1}(t), x_{N-u_1+1}^*(t), y_{v_2+1}^*(t), x_{N-v_1+1}(t)\}, & \text{when } u_1 \ne 0, v_1 \ne 0 \end{cases} \quad (5)$$

Denote the unique decomposition of u and v as

$$\begin{cases} u = u_1 + u_2(N+1) \\ v - N + 1 = v_1 + v_2 N, & N \le v \le N - 1 + MN \\ v - N + 1 - MN = v_1 + 2v_2, & N + MN \le v \le N + MN + 2M - 3 \end{cases} \quad (6)$$

where $0 \le u_1 \le N$, $1 \le v_1 \le N$ for $N \le v \le N - 1 + MN$ and $1 \le v_1 \le 2$ for $N + MN \le v \le N + MN + 2M - 3$. Then, we can construct $\mathbf{C}_2$ by

$\mathbf{C}_2(u,v) =$

$$\begin{cases} cum\{y_M(t), y_{M-u_2}^*(t), x_v(t), x_1(t)\}, & \text{if } u_1 = 0, v \le N - 1 \\ cum\{y_M(t), y_{M-u_2}^*(t), y_{v_2+1}(t), x_{v_1}(t)\}, & \text{if } u_1 = 0, N \le v \le N - 1 + MN \\ cum\{y_M(t), y_{M-u_2}^*(t), y_{M-2+v_1}(t), y_{2+v_2}(t)\}, & \text{if } u_1 = 0, N + MN \le v \le N + MN + 2M - 3 \\ cum\{y_{u_2+1}(t), x_{N-u_1+1}^*(t), x_v(t), x_1(t)\}, & \text{if } u_1 \ne 0, v \le N - 1 \\ cum\{y_{u_2+1}(t), x_{N-u_1+1}^*(t), y_{v_2+1}(t), x_{v_1}(t)\}, & \text{if } u_1 \ne 0, N \le v \le N - 1 + MN \\ cum\{y_{u_2+1}(t), x_{N-u_1+1}^*(t), y_{M-2+v_1}(t), y_{2+v_2}(t)\}, & \text{if } u_1 \ne 0, N + MN \le v \le N + MN + 2M - 3 \end{cases} \quad (7)$$

Denote the unique decomposition of u and v as

$$\begin{cases} v = v_1 + v_2(N+1) \\ u - N + 1 = u_1 + u_2 N, & N \le u \le N - 1 + MN \\ u - N + 1 - MN = u_1 + 2u_2, & N + MN \le u \le N + MN + 2M - 3 \end{cases} \quad (8)$$

where $0 \le v_1 \le N$, $1 \le u_1 \le N$ for $N \le u \le N - 1 + MN$ and $1 \le u_1 \le 2$ for $N + MN \le u \le N + MN + 2M - 3$. Then, we can construct $\mathbf{C}_3$ by

$\mathbf{C}_3(u,v) =$

$$\begin{cases} cum\{x_u^*(t), x_1^*(t), y_M^*(t), y_{M-v_2}(t)\}, & \text{if } u \le N - 1, v_1 = 0 \\ cum\{y_{u_2+1}^*(t), x_{u_1}^*(t), y_M^*(t), y_{M-v_2}(t)\}, & \text{if } N \le u \le N - 1 + MN, v_1 = 0 \\ cum\{y_{M-2+u_1}^*(t), y_{2+u_2}^*(t), y_M^*(t), y_{M-v_2}(t)\}, & \text{if } N + MN \le u \le N + MN + 2M - 3, v_1 = 0 \\ cum\{x_u^*(t), x_1^*(t), y_{v_2+1}^*(t), x_{N-v_1+1}(t)\}, & \text{if } u \le N - 1, v_1 \ne 0 \\ cum\{y_{u_2+1}^*(t), x_{u_1}^*(t), y_{v_2+1}^*(t), x_{N-v_1+1}(t)\}, & \text{if } N \le u \le N - 1 + MN, v_1 \ne 0, \\ cum\{y_{M-2+u_1}^*(t), y_{2+u_2}^*(t), y_{v_2+1}^*(t), x_{N-v_1+1}(t)\}, & \text{if } N + MN \le u \le N + MN + 2M - 3, v_1 \ne 0, \end{cases} \quad (9)$$

Denote the unique decomposition of u and v as

$$\begin{cases} u - N + 1 = u_1 + u_2 N, & N \le u \le N - 1 + MN \\ u - N + 1 - MN = u_1 + 2u_2, & N + MN \le u \le N + MN + 2M - 3 \\ v - N + 1 = v_1 + v_2 N, & N \le v \le N - 1 + MN \\ v - N + 1 - MN = v_1 + 2v_2, & N + MN \le v \le N + MN + 2M - 3 \end{cases} \tag{10}$$

where $1 \le u_1, v_1 \le N$ for $N \le u, v \le N - 1 + MN$, and $1 \le u_1, v_1 \le 2$ for $N + MN \le u$, $v \le N + MN + 2M - 3$. Then, we can construct $\mathbf{C}_4$ by

$\mathbf{C}_4(u, v) =$
$$\begin{cases} cum\{x_u^*(t), x_1^*(t), x_v(t), x_1(t)\}, & \text{if } u \le N - 1, v \le N - 1 \\ cum\{x_u^*(t), x_1^*(t), y_{v_2+1}(t), x_{v_1}(t)\}, & \text{if } u \le N - 1, N \le v \le N - 1 + MN \\ cum\{x_u^*(t), x_1^*(t), y_{M-2+v_1}(t), y_{2+v_2}(t)\}, & \text{if } u \le N - 1, N + MN \le v \le N + MN + 2M - 3 \\ cum\{y_{u_2+1}^*(t), x_{u_1}^*(t), x_v(t), x_1(t)\}, & \text{if } N \le u \le N - 1 + M, v \le N - 1 \\ cum\{y_{u_2+1}^*(t), x_{u_1}^*(t), y_{v_2+1}(t), x_{v_1}(t)\}, & \text{if } N \le u \le N - 1 + M, N \le v \le N - 1 + MN \\ cum\{y_{u_2+1}^*(t), x_{u_1}^*(t), y_{M-2+v_1}(t), y_{2+v_2}(t)\}, & \text{if } N \le u \le N - 1 + M, N + MN \le v \le N + MN + 2M - 3 \\ cum\{y_{M-u_1}^*(t), y_{2+u_2}^*(t), x_v(t), x_1(t)\}, & \text{if } N + MN \le u \le N + MN + 2M - 3, v \le N - 1 \\ cum\{y_{M-u_1}^*(t), y_{2+u_2}^*(t), y_{v_2+1}(t), x_{v_1}(t)\}, & \text{if } N + MN \le u \le N + MN + 2M - 3, N \le v \le N - 1 + MN \\ cum\{y_{M-u_1}^*(t), y_{2+u_2}^*(t), y_{M-2+v_1}(t), y_{2+v_2}(t)\}, & \text{if } N + MN \le u \le N + MN + 2M - 3, N + MN \le v \le N + MN + 2M - 3 \end{cases} \tag{11}$$

Denote $\tilde{\mathbf{C}}_2$ as the matrix after moving the $(N + MN + 2M - 4)$th column of $\mathbf{C}_2$. Denote $\tilde{\mathbf{C}}_3$ as the matrix after moving the $(N + MN + 2M - 4)$th row of $\mathbf{C}_3$. Denote $\tilde{\mathbf{C}}_4$ as the matrix after moving the $(N + MN + 2M - 4)$th column and the $(N + MN + 2M - 4)$th row and of $\mathbf{C}_4$.

We can form a high-order matrix $\mathbf{C} \in C^{(2MN+3M+N-6)\times(2MN+3M+N-6)}$ as

$$\mathbf{C} = \begin{bmatrix} \mathbf{C}_1 & \tilde{\mathbf{C}}_2 \\ \tilde{\mathbf{C}}_3 & \tilde{\mathbf{C}}_4 \end{bmatrix} \tag{12}$$

Denote a vector $\tilde{\mathbf{a}}_2(\theta_k) \in C^{(N+MN+2M-3)\times 1}$ as

$$\tilde{\mathbf{a}}_2(\theta_k) = \begin{bmatrix} \mathbf{a}_1(\theta_k) \\ \mathbf{b}(\theta_k) \otimes \mathbf{a}(\theta_k) \\ \mathbf{b}_2(\theta_k) \otimes \mathbf{b}_3(\theta_k) \end{bmatrix} \tag{13}$$

where $\mathbf{a}_1(\theta_k) = [\mathbf{a}(\theta_k)]_{1:N-1}$, $\mathbf{b}_2(\theta_k) = [\mathbf{b}(\theta_k)]_{2:M}$ and $\mathbf{b}_3(\theta_k) = [\mathbf{b}(\theta_k)]_{M-1:M}$.

Using $\tilde{\mathbf{a}}_2(\theta_k)$, denote the vector $\bar{\mathbf{a}}_2(\theta_k) \in C^{(N+MN+2M-4)\times 1}$ after removing the $(N+MN+2M-4)$th element of $\tilde{\mathbf{a}}_2(\theta_k)$.

From Eqs. (4)–(12), matrix $\mathbf{C}$ can be expressed as a product of three matrices as

$$\mathbf{C} = \begin{bmatrix} \bar{\mathbf{A}}_1 \mathbf{S}_0 \bar{\mathbf{A}}_1^H & \bar{\mathbf{A}}_1 \mathbf{S}_0 (\mathbf{\Phi}^*)^H \bar{\mathbf{A}}_2^T \\ \bar{\mathbf{A}}_2^* \mathbf{\Phi}^* \mathbf{S}_0 \bar{\mathbf{A}}_1^H & \bar{\mathbf{A}}_2 \mathbf{S}_0 \bar{\mathbf{A}}_2^T \end{bmatrix} = \begin{bmatrix} \bar{\mathbf{A}}_1 \\ \bar{\mathbf{A}}_2^*(\mathbf{\Phi}^*) \end{bmatrix} \mathbf{S}_0 \begin{bmatrix} \bar{\mathbf{A}}_1^H & (\mathbf{\Phi}^*)^H \bar{\mathbf{A}}_2^T \end{bmatrix} \tag{14}$$

where $\bar{\mathbf{A}}_1 = [\bar{\mathbf{a}}_1(\theta_1), \bar{\mathbf{a}}_1(\theta_2), \cdots, \bar{\mathbf{a}}_1(\theta_K)]$, $\bar{\mathbf{A}}_2 = [\bar{\mathbf{a}}_2(\theta_1), \bar{\mathbf{a}}_2(\theta_2), \cdots, \bar{\mathbf{a}}_2(\theta_K)]$, $\bar{\mathbf{a}}_1(\theta_k) = [1, e^{-i\Delta \sin(\theta_k)}, \cdots,$ $e^{-i\Delta(MN+M-3)\sin(\theta_k)}]^T \in C^{(MN+M-2)\times 1}$ and $\mathbf{S}_0 = \text{diag}\{\mathbf{s}_{01}, \mathbf{s}_{02}, \cdots, \mathbf{s}_{0K}\}$.

3.2. NC-MUSIC Based on FOC

Implementing EVD on the matrix $\mathbf{C}$ yields

$$\mathbf{C} = \mathbf{U}_s \Sigma_s \mathbf{U}_s^H + \mathbf{U}_n \Sigma_n \mathbf{U}_n^H \tag{15}$$

where Σ_s denotes a $K \times K$ diagonal matrix formed by K largest eigenvalues, and Σ_n denotes a diagonal matrix formed by the rest $2MN + 3M + N - 6 - K$ smaller eigenvalues. Matrix $\mathbf{U}_s$ is composed by the eigenvectors corresponding to the K largest eigenvalues, and $\mathbf{U}_n$ consists of the rest eigenvectors.

Denote matrix $\bar{\mathbf{A}} = \left[\ (\bar{\mathbf{A}}_1)^T\ \ (\bar{\mathbf{A}}_2^*(\mathbf{\Phi}^*))^T\ \right]^T$, and the relation between $\bar{\mathbf{A}}$ and $\mathbf{U}_n$ can be formulated as

$$\bar{\mathbf{A}}^H \mathbf{U}_n = 0 \tag{16}$$

Divide $\mathbf{U}_n$ into two parts

$$\mathbf{U}_n = \left[\begin{array}{c} \mathbf{U}_{n1} \\ \mathbf{U}_{n2} \end{array} \right] \tag{17}$$

where $\mathbf{U}_{n1} \in C^{(MN+M-2)\times K}$ and $\mathbf{U}_{n2} \in C^{(MN+N+2M-4)\times K}$.

As the traditional NC-MUSIC algorithm [4], we can get the estimation of $\boldsymbol{\theta} = [\theta_1, \theta_2, \cdots, \theta_K]$ by minimizing the cost function $f(\theta, \phi)$

$$
\begin{aligned}
f(\theta, \phi) &= \left[\begin{array}{c} \bar{\mathbf{a}}_1(\theta) \\ e^{j\phi}\bar{\mathbf{a}}_2^*(\theta) \end{array} \right]^H \left[\begin{array}{c} \mathbf{U}_{n1} \\ \mathbf{U}_{n2} \end{array} \right] \left[\ \mathbf{U}_{n1}^H\ \ \mathbf{U}_{n2}^H\ \right] \left[\begin{array}{c} \bar{\mathbf{a}}_1(\theta) \\ e^{j\phi}\bar{\mathbf{a}}_2^*(\theta) \end{array} \right] \\
&= \left[\begin{array}{c} 1 \\ e^{j\phi} \end{array} \right]^H \left[\begin{array}{cc} \bar{a}_1(\theta) & 0 \\ 0 & \bar{a}_2^*(\theta) \end{array} \right]^H \left[\begin{array}{cc} U_{n1}U_{n1}^H & U_{n1}U_{n2}^H \\ U_{n2}U_{n1}^H & U_{n2}U_{n2}^H \end{array} \right] \left[\begin{array}{cc} \bar{a}_1(\theta) & 0 \\ 0 & \bar{a}_2^*(\theta) \end{array} \right] \left[\begin{array}{c} 1 \\ e^{j\phi} \end{array} \right]
\end{aligned} \tag{18}
$$

Let $\frac{\partial f(\theta, \phi)}{\partial \phi} = 0$, we can get the new cost function $g(\theta)$ as [4]

$$g(\theta) = \bar{\mathbf{a}}_1^H \mathbf{U}_{n1} \mathbf{U}_{n1}^H \bar{\mathbf{a}}_1 + \bar{\mathbf{a}}_2^T \mathbf{U}_{n2} \mathbf{U}_{n2}^H \bar{\mathbf{a}}_2^* - 2 \left\| \bar{\mathbf{a}}_1^H \mathbf{U}_{n1} \mathbf{U}_{n2}^H \bar{\mathbf{a}}_2^* \right\| \tag{19}$$

At last, we can get the estimation of $\boldsymbol{\theta} = [\theta_1, \theta_2, \cdots, \theta_K]$ by 1-D peak search for $1/g(\theta)$.

4. SIMULATION RESULTS

In this section, two groups of simulation experiments are proposed to evaluate the performance of proposed NC-MUSIC with nested array. The proposed NC-MUSIC is compared with NC-MUSIC based on SOS [4] and NC-MUSIC based on FOC [15]. Let $M = 5$, $N = 4$, $d = \lambda/2$, and the number of elements is $N + M - 1 = 8$. So we employ an 8-element uniform linear array for the other two algorithms. We fix the search interval at $0.1°$ for the two groups of experiments and assume that all
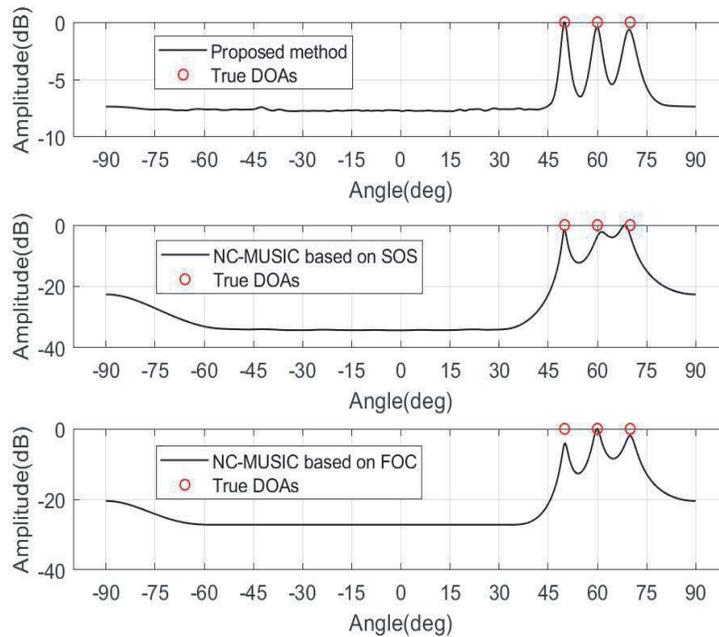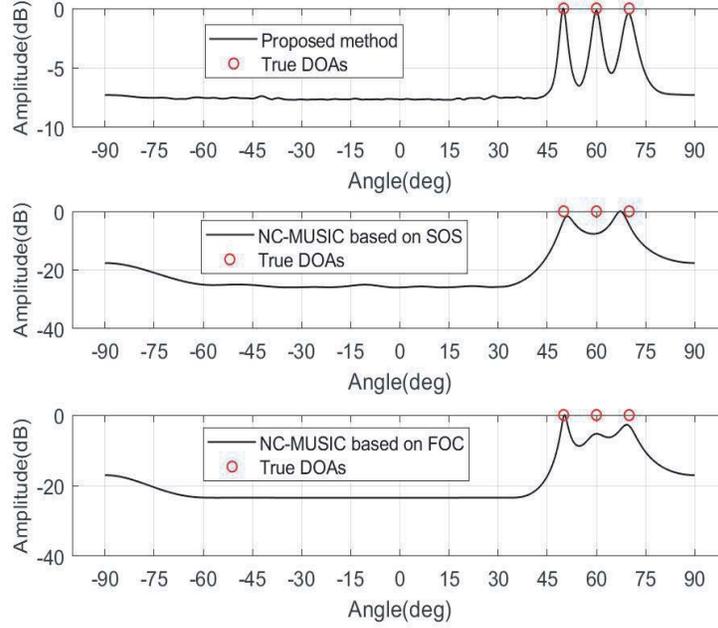

Figure 2. Spatial spectrums of three methods with $\text{SNR} = 5\,\text{dB}$ for $[\theta_1, \theta_2, \theta_3] = [50°, 60°, 70°]$.
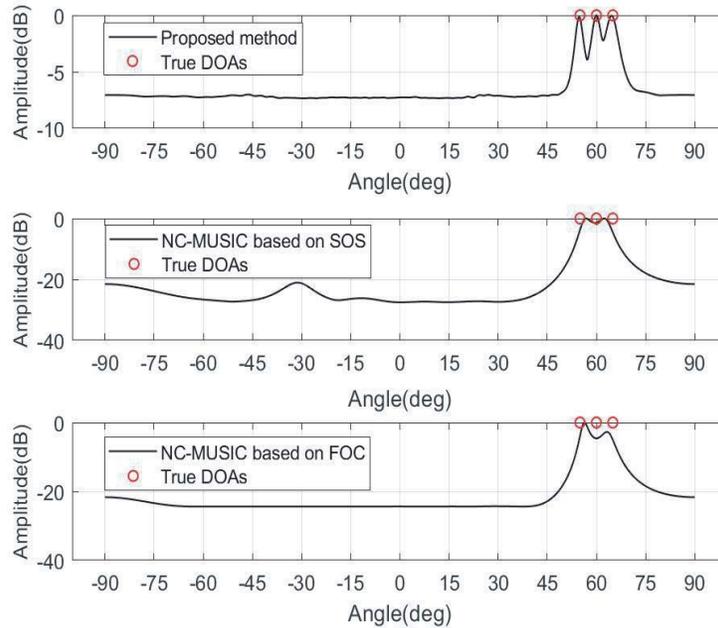
the incident signals have the biggest non-circularity. Define the root-mean-square error (RMSE) of the angle estimation as

$$\text{RMSE} = \sqrt{\frac{1}{KJ} \sum_{i=1}^{J} \sum_{k=1}^{K} \left(\hat{\theta}_{kj} - \theta_k\right)^2} \tag{20}$$

where $J = 200$, and $\hat{\theta}_{kj}$ is the estimation of the kth signal in the jth Monte Carlo trial.

Figure 3. Spatial spectrums of three methods with SNR $= 0\,\text{dB}$ for $[\theta_1, \theta_2, \theta_3] = [50°, 60°, 70°]$.

Figure 4. Spatial spectrums of three methods with SNR $= 0\,\text{dB}$ for $[\theta_1, \theta_2, \theta_3] = [55°, 60°, 65°]$.

4.1. Experiment 1

In this experiment, we show the spatial spectrums of three NC-MUSIC algorithms. Received data by 500 snapshots are used to estimate the covariance matrix and FOC matrix. Firstly, we consider the condition that three signals are from the directions $[50°, 60°, 70°]$. Fig. 2 shows the spatial spectrums of three NC-MUSIC algorithms with 5 dB SNR. Fig. 3 shows the comparison of spatial spectrums of three NC-MUSIC algorithms with SNR being changed into 0 dB. Then, we consider the condition that three signals are from the directions $[55°, 60°, 65°]$. The spatial spectrums of three algorithms with 0 dB SNR are depicted in Fig. 4. The results shown in the three figures reflect that the proposed method can distinguish the three angles clearly under three situations. However, the other two methods only can distinguish the three angles under the first situation.
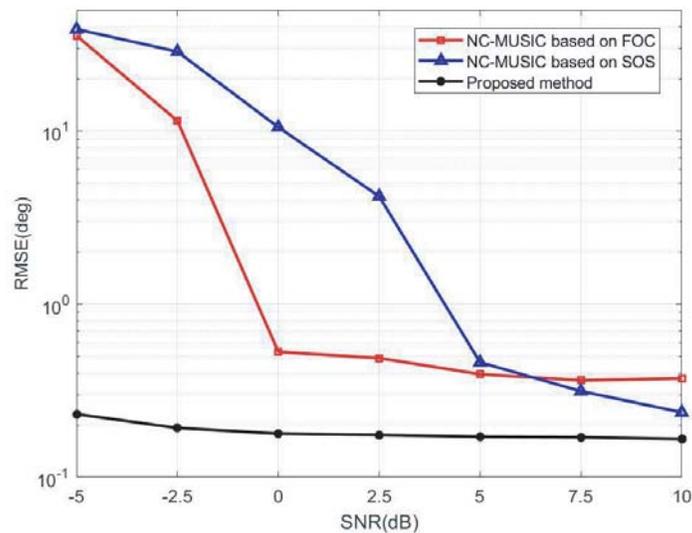

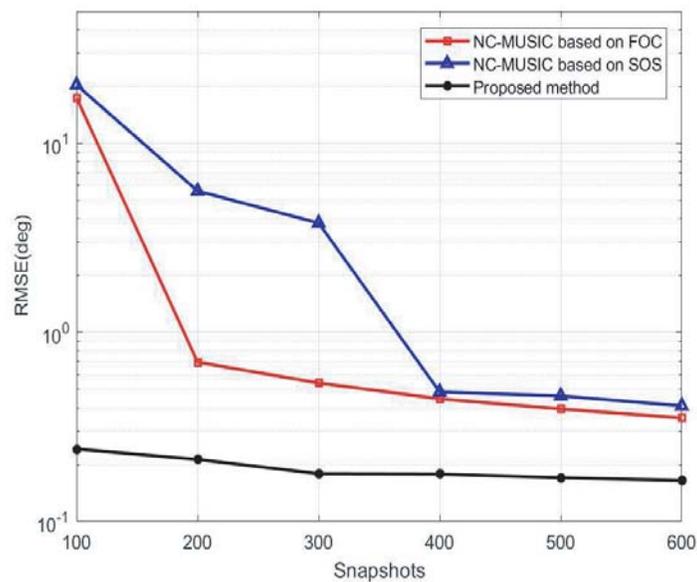**Figure 5.** RMSEs of DOA estimates versus SNR.

Figure 6. RMSEs of DOA estimates versus snapshots.

4.2. Experiment 2

In the second experiment, we compare the estimation accuracy of three NC-MUSIC algorithms. Three signals are located at the directions $[50°, 60°, 70°]$. Firstly, the number of snapshots is fixed at 500 with the SNR changing from $-5\,\mathrm{dB}$ to $10\,\mathrm{dB}$. The RMSEs versus SNR are described in Fig. 5. Then, the SNR is fixed at $5\,\mathrm{dB}$ with the number of snapshots changing from 100 to 600. The RMSEs of three methods with regard to snapshots are displayed in Fig. 6. From Fig. 5 and Fig. 6, we can know that the estimation accuracy of proposed algorithm is better than the other two algorithms, particularly for the lower SNR and snapshots scene.

5. CONCLUSION

In this paper, we have presented a FOC-based NC-MUSIC algorithm for the DOA estimation of noncircular signals by using nested array. The process of constructing FOC matrix is described in detail. The proposed algorithm shows better angular resolution and precision than some classical NC-MUSIC algorithms due to the extension of array aperture, especially in low SNR and snapshots scene.

ACKNOWLEDGMENT

REFERENCES

1. Zhang, X., X. Gao, G. Feng, and D. Xu, "Blind joint DOA and DOD estimation and identifiability results for MIMO radar with different transmit/receive array manifolds," *Progress In Electromagnetics Research B*, Vol. 18, 101–119, 2009.

2. Katkovnik, V., S. M. Lee, and H. Y. Kim, "Performance study of the minimax robust phased array for wireless communications," *IEEE Transactions on Communications*, Vol. 54, No. 4, 608–613, 2006.

3. Zhang, X. F., M. Zhou, H. Chen, and F. J. Li, "Two-dimensional DOA estimation for acoustic vector-sensor array using a successive MUSIC," *Multidimensional System and Signal Processing*, Vol. 25, No. 3, 583–600, 2014.

4. Gounon, P., C. Adnet, and J. Galy, "Angular localization for noncircular signals," *Traitement du Signal*, Vol. 15, No. 1, 17–24, 1998.

5. Charge, P., Y. Wang, and J. Saillard, "A noncircular sources direction finding method using polynomial rooting," *Signal Processing*, Vol. 81, No. 8, 1765–1770, 2001.

6. Gao, F. F., A. Nallanathan, and D. Y. Wang, "Improved MUSIC under the coexistence of both circular and noncircular sources," *IEEE Transactions on Signal Processing*, Vol. 56, No. 7, 3033–3038, 2008.

7. Si, W. J., T. Zhu, and Y. M. Zhang, "DOA estimation in solving mixed circular and non-circular incident signals," *Systems Engineering and Electronics*, Vol. 34, 882–886, 2012.

8. Haardt, M. and F. Romer, "Enhancements of unitary ESPRIT for noncircular sources," *The Proceeding of 2004 IEEE International Conference on Acoustics, Speech and Signal Processing*, Vol. 2, 101–104, Montreal, Quebec, Canada, 2004.

9. Haardt, M. and A. J. Nossek, "Unitary ESPRIT: How to obtain increased estimation accuracy with a reduced computational burden," *IEEE Transaction on Signal Processing*, Vol. 43, No. 5, 1232–1242, 1995.

10. Liu, J., T. Z. Huang, and Y. Y. Zhou, "Extended propagator method for direction estimation of noncircular signals," *Signal Processing*, Vol. 24, No. 4, 556–560, 2008.

11. Liu, Z. X., Y. Li, M. A. Song, and J. Liu, "Extended propagator method for noncircular signals estimation with polynomial rooting," *Journal of Air Force Engineering University*, Vol. 12, No. 4, 58–63, 2011.

12. Gan, L., F. J. Gu, and P. Wei, "Estimation of 2-D DOA for noncircular sources using simultaneous SVD technique," *IEEE Antennas Wireless and Propagate Letters*, Vol. 7, 385–388, 2008.

13. Porat, B. and B. Friedlander, "Direction finding algorithms based on high-order statistics," *IEEE Transactions on Signal Processing*, Vol. 39, No. 9, 2016–2024, 1991.

14. Dogan, M. C. and J. M. Mendel, "Application of cumulants to array processing — Part I: Aperture extension and array calibration," *IEEE Transactions on Signal Processing*, Vol. 43, No. 5, 1200–1216, 1995.

15. Liu, J., T. Z. Huang, and Y. Y.Zhou, "A new forth-order direction finding algorithm for noncircular signals," *Journal of Electronics and Information Technology*, Vol. 30, 876–880, 2008.

16. Camps, A. and A. Cardama, "Infantes, D. Synthesis of large low redundancy linear arrays," *IEEE Transactions on Antennas and Propagation*, Vol. 49, No. 12, 1881–1883, 2001.

17. Vaidyanathan, P. P. and P. Pal, "Sparse sensing wth co-prime samplers and arrays," *IEEE Transactions on Signal Processing*, Vol. 59, No. 2, 573–586, 2010.

18. Liu, S., L. Yang, D. Li, H. L. Cao, and Q. P. Jiang, "2D DOA estimation for noncircular sources using L-shaped sparse array," *Multidimensional Systems & Signal Processing*, Vol. 29, No. 2, 489–502, 2018.

19. Iizuka, Y. and K. Ichige, "Extension of nested array for large aperture and high degree of freedom," *IEICE Communications Express*, Vol. 6, No. 6, 381–386, 2017.

20. Yang, M., L. Sun, X. Yuan, and B. X. Chen, "Improved nested array with hole-free DCA and more degrees of freedom," *Electronics Letters*, Vol. 52, No. 25, 2068–2070, 2016.

21. Huang, H., B. Liao, X. Wang, X. S. Guo, and J. Huang, "A new nested array configuration with increased degrees of freedom," *IEEE Access*, Vol. 6, 1490–1497, 2018.